

Quantum Semi-Random Forests for Qubit-Efficient Recommender Systems

Azadeh Alavi*, Fatemeh Kouchmeshki†, Abdolrahman Alavi†, Yongli Ren*, Jiayang Niu*

*RMIT University, Melbourne, Australia

Email: {azadeh.alavi, yongli.ren, s4068570}@rmit.edu.au

†Pattern Recognition Pty. Ltd., Melbourne, Australia

Email: {admin@pr2aid.com, rahmanalavi1944@gmail.com}

First and second authors contributed equally to this work

Abstract—Modern recommenders describe each item with hundreds of sparse semantic tags, yet most quantum pipelines still map one qubit per tag, demanding well beyond one hundred qubits, far out of reach for current noisy-intermediate-scale quantum (NISQ) devices and prone to deep, error-amplifying circuits. We close this gap with a three-stage hybrid machine learning algorithm that compresses tag profiles, optimizes feature selection under a fixed qubit budget via QAOA, and scores recommendations with a Quantum semi-Random Forest (QsRF) built on just five qubits, while performing similarly to the state-of-the-art methods. Leveraging SVD sketching and k-means, we learn a 1 000-atom dictionary (>97 % variance), then solve a 20×20 QUBO via depth-3 QAOA to select 5 atoms. A 100-tree QsRF trained on these codes matches full-feature baselines on ICM-150/500.

Index Terms—recommender systems, Dictionary Learning, QAOA, Bagged trees, Quantum machine learning, hybrid machine learning recommender systems, Dictionary Learning, QAOA, Bagged trees, Quantum machine learning, hybrid machine learningR

I. INTRODUCTION & RELATED WORK

Modern content platforms such as *Netflix*, *Amazon* and *TikTok* describe every item with hundreds of sparse semantic tags. Identifying the smallest subset that preserves ranking quality is NP-hard, and naïvely mapping one qubit to one tag quickly surpasses the limits of Noisy-Intermediate-Scale-Quantum (NISQ) hardware. To compress this combinatorial explosion, recent hybrid pipelines formulate feature selection as a Quadratic Unconstrained Binary Optimisation (QUBO) and delegate the search to quantum annealers [1], [2] or shallow gate-based circuits [3]. Nevertheless, the entire 150-tag space in the smallest QuantumCLEF split is still embedded onto hardware with limited connectivity, leading to deep, error-prone circuits.

Historically, recommender systems relied on dense latent factor models whose dimensions are hard to interpret. In contrast, dictionary learning provides compact and inherently sparse representations. Early large-scale work by Mensch *et al.* [4] introduced a K-SVD-style factorisation that scales to terabyte user-item matrices, while Kartoglu and Spratling [5] demonstrated that structured sparse coding can rival dense baselines in both rating prediction and top- N ranking with far

fewer parameters. Such results suggest that a well-chosen set of interpretable atoms can replace raw tags without sacrificing accuracy—an observation we exploit *before* invoking quantum search.

Quantum feature selection has so far moved along two strands. On the one hand, mutual-information and counterfactual criteria have been encoded directly into QUBO matrices and solved with either quantum annealing or the Quantum Approximate Optimisation Algorithm (QAOA) [2], [6], [7]. On the other hand, recursive variants such as RQAOA iteratively fix strongly correlated variables to keep qubit counts manageable, albeit at the cost of multiple quantum evaluations and heuristic rounding [8]. Despite these innovations, published studies still operate on only 10–20 features and remain bottlenecked by the *linear* growth in qubit demand.

Meanwhile, the QAOA landscape itself has matured from proof-of-concepts to medium-scale demonstrations. Harrigan *et al.* executed depth-2 QAOA on 23 superconducting qubits, validating theoretical predictions but exposing depth-related locality issues [9]. Follow-up work introduced non-local mixers, parameter-transfer heuristics and hybrid decomposition schemes, yet a definitive advantage over classical solvers is still elusive. Ferrari Dacrema *et al.* systematically compared QPU, hybrid, simulated-annealing and tabu-search solvers on up to 5 000 features and found quantum approaches merely *competitive* once problem sizes required decomposition [10]. Consequently, qubit-efficient representations remain the critical enabler for any near-term quantum recommender.

A. Why Gate-based QAOA over Quantum Annealing?

Quantum annealers excel at native Chimera/Pegasus topologies but incur a *minor-embedding* overhead for fully-connected QUBOs: a single logical variable is mapped to a ferromagnetically coupled *chain* of physical qubits whose expected length scales as $\mathcal{O}(\sqrt{M})$ [11]. For our 20×20 performance-driven QUBO this would raise the effective budget from 5 logical qubits to >60 physical qubits—even before error-correcting replica chains are considered. Chain breaks further degrade solution quality and require post-processing heuristics [12].

arXiv:2508.00027v1 [quant-ph] 30 Jul 2025

Gate-based devices avoid minor embedding: the five logical qubits are mapped one-to-one onto hardware, and all-to-all connectivity is emulated by SWAP insertions whose count grows only $\mathcal{O}(k^2)$ with $k = 5$. Although recent studies show that annealers outperform one-round QAOA on ~ 100 -qubit Ising benchmarks [11], deeper ($p \geq 3$) QAOA with noise-aware angle optimisation starts to close that gap while providing algorithmic flexibility—e.g. exact cardinality constraints via the penalty term in Eq.(3). Moreover, QAOA circuits can be simulated end-to-end on GPUs, enabling rapid hyperparameter sweeps that are infeasible on remotely accessed annealers.

In short, the **5-qubit** gate-based route offers (i) zero embedding overhead, (ii) explicit control over depth and mixer choice, and (iii) straightforward integration with classical autotuners—making it the pragmatic option for our qubit-budget scenario.

B. Our Contribution

In this work, we show that the item–tag matrix is *highly low-rank*: the top 32 singular vectors already capture more than 97 % of the training variance [13]. Leveraging this structure, we compress the 150-dimensional Euclidean space into only five dictionary atoms and then conduct feature selection with a depth-3 QAOA that requires exactly five qubits. A bagged ensemble of shallow decision trees—dubbed a *Quantum semi-Random Forest* (QsRF)—recovers the non-linearity lost during compression and achieves competitive ranking accuracy on the QuantumCLEF ICM–150 benchmark.

- 1) We introduce a three-stage hybrid pipeline—SVD sketching, k-means clustering, and Mini-Batch Dictionary Learning—that builds a 1000-atom dictionary capturing > 97% of tag-profile variance, enabling a $\approx 90\%$ reduction in qubit usage.
- 2) We derive a five-qubit QUBO whose objective is proportional to the incremental Δ -nDCG on bootstrap subsamples; a depth-3 QAOA then selects the optimal 5-atom subset under a strict qubit budget.
- 3) We propose a Quantum semi-Random Forest (QsRF) ensemble of 100 shallow decision trees (10 runs \times 10 trees) trained on those 5-dimensional codes, achieving superior nDCG@10, AUC, and Log-Loss compared to state-of-the-art methods while using only five qubits.
- 4) We perform an ablation study over dictionary rank, bootstrap size, and QAOA depth, and demonstrate an order-of-magnitude ($\approx 10\times$) reduction in end-to-end runtime versus CAQUBO and MIQUBO.



Fig. 1: End-to-end pipeline: dictionary learning compresses

...

II. METHODOLOGY

Let $X \in \mathbb{R}^{N \times M}$ be the TF-IDF matrix of N user–item interactions and $M = 150$ original tags. We aim to learn a compact dictionary $D_k \in \mathbb{R}^{M \times k}$ with $k = 5$ atoms such that (i) D_k reconstructs X with minimal information loss and (ii) the selected atoms maximise the ranking metric nDCG@10. Figure 1 and Algorithm 1 outline the three main stages; the present section makes each step mathematically explicit.

A. Stage 1 — Low-rank dictionary learning

(a) Randomised SVD. Following Halko *et al.* [13], we first compute a rank- d sketch $Z = XV_d$ with $d = 32$, where $V_d \in \mathbb{R}^{M \times d}$ contains the top right singular vectors. This step reduces both memory and time complexity from $\mathcal{O}(NM)$ to $\mathcal{O}(Nd^2)$ while preserving > 97% of the Frobenius energy.

(b) MiniBatch k -Means. The rows of Z are clustered into $K = 50$ disjoint sets $\{\mathcal{C}_1, \dots, \mathcal{C}_K\}$ via MiniBatch k -Means. Clustering exposes local linear structure and allows sub-dictionaries to be trained in parallel.

(c) Sparse coding within each cluster. For cluster c , we learn a sub-dictionary $D_c \in \mathbb{R}^{M \times A}$ with $A = 20$ atoms by solving

$$\min_{D_c, \Theta_c} \frac{1}{2} \|Z_{\mathcal{C}_c} - \Theta_c D_c^\top\|_F^2 + \lambda \|\Theta_c\|_1, \quad (1)$$

where Θ_c stores the sparse codes and λ controls sparsity. We adopt an alternating scheme identical to K-SVD [4], but replace the L_0 projector with LARS-Lasso updates for faster convergence. The union $D = [D_1 \parallel \dots \parallel D_K] \in \mathbb{R}^{M \times 1000}$ serves as our master atom pool.

B. Stage 2 — Performance-driven importance scores

For each atom j , let $\delta_u^{(j)} = \text{nDCG@10}(u) - \text{nDCG@10}^{(-j)}(u)$ denote the drop in ranking quality for user u when the atom is removed. Averaging over a bootstrap \mathcal{B} of 20% of the training rows yields the *performance-driven* weight

$$w_j = \frac{1}{|\mathcal{B}|} \sum_{u \in \mathcal{B}} \delta_u^{(j)}. \quad (2)$$

The $K_{\text{top}} = 20$ highest-scoring atoms constitute the candidate set \mathcal{T} that will be fed to the quantum search.

C. Stage 3 — Five-qubit QUBO and depth-3 QAOA

(a) QUBO formulation. Let $z \in \{0, 1\}^{K_{\text{top}}}$ be a binary mask over \mathcal{T} and $k = 5$ the desired budget. We define the energy

$$E(z) = - \sum_{j=1}^{K_{\text{top}}} w_j z_j + \mu (\sum_j z_j - k)^2, \quad (3)$$

with penalty $\mu = \sim 10^3$ to enforce $\sum_j z_j = k$. Expanding (3) as $z^\top Q z$ yields a dense 20×20 QUBO matrix $Q = -\text{diag}(w) + \mu \mathbf{1}\mathbf{1}^\top$ that fits comfortably on five logical qubits.

(b) **QAOA ansatz.** We employ the depth- $p = 3$ Quantum Approximate Optimisation Algorithm [14]. The cost Hamiltonian is $\mathcal{H}_C = \sum_{i \leq j} Q_{ij} Z_i Z_j$ and the mixer $\mathcal{H}_M = \sum_j X_j$. The variational circuit alternates the unitaries $\exp(-i\gamma_\ell \mathcal{H}_C)$ and $\exp(-i\beta_\ell \mathcal{H}_M)$ for $\ell = 1, \dots, p$. Parameters $(\gamma, \beta) \in \mathbb{R}^{2p}$ are optimised on the validation split with Simultaneous Perturbation Stochastic Approximation (SPSA) [15] using 128 shots per objective evaluation. Measurement returns a bit-string \hat{z} ; if $\sum_j \hat{z}_j = k$ the corresponding atoms are accepted, otherwise we fall back to the top- k by w_j .

D. Stage 4 — Quantum semi-Random Forest (QsRF)

Given the final five-dimensional codes $\check{Z} = X D_k$, we train an ensemble of $T = 200$ decision trees under bagging [16]. Each tree receives a bootstrap of the training rows and a random perturbation of the feature indices, mimicking the stochasticity of classical Random Forests while preserving the extremely low feature count delivered by the quantum stage. At inference time the predicted click-through probability for a user-item pair is the arithmetic mean over all tree outputs.

E. Complexity remarks

Time. Randomised SVD costs $\mathcal{O}(N d^2)$; dictionary learning across clusters is $\mathcal{O}(N_{\text{iter}} |Z| A)$ with $A = 20$ fixed. QAOA incurs $\mathcal{O}(p 2^k)$ state-vector updates but with $k = 5$ and $p = 3$ this is negligible. Tree training scales linearly with N and T .

Space. The memory footprint peaks at the 1000-atom matrix D (≈ 0.8 MB in single precision) plus the five-qubit state vector during QAOA optimisation. No step exceeds GPU memory limits on a single RTX A6000. In practice the end-to-end pipeline is lightweight. On an 8-core laptop (Apple M2, 32 GB RAM) dictionary learning dominates with one global 1 000-atom pass plus ten fine-tune passes over at most five atoms each; a single mini-batch update costs $\mathcal{O}(b M A)$ with $b = 2048$, $M \approx 150$ and $A \leq 5$, and the entire phase completes in ~ 6 min. Sparse encoding solves 110 LARS-Lasso problems per run, each $\mathcal{O}(M A)$ per sample, finishing in < 90 s when parallelised across all cores. QAOA optimisation (depth 3, 20×20 QUBO) is negligible ten SPSA runs add < 60 s. Finally, training 100 depth-8 trees on the 5-dimensional codes is trivial (~ 20 s). Overall, the full train-validate-test pipeline takes 8–12 min wall-clock, well within typical academic time budgets.

F. Computational Complexity & Runtime

All QAOA circuits were executed on the PennyLane simulator [17] using default noise-free backends; we plan to validate our approach on real quantum hardware as it becomes available. The dominant costs are:

- **Dictionary learning:** one global 1000-atom pass + $10 \times$ one-pass fine-tunes (5 atoms). Each minibatch update is $\mathcal{O}(b M A)$ with $b = 2048$, $M \approx 150$, $A \leq 5$.
- **Sparse encoding:** 110 LASSO-LARS solves per run (train+test), each $\mathcal{O}(M A)$ per sample; we parallelize with `n_jobs=-1`.

Algorithm 1: QsRF-QAOA five-qubit recommender pipeline

Input: TF-IDF matrix $X \in \mathbb{R}^{N \times 150}$, implicit-feedback labels y
Output: ranked item list per user

- 2 // Dictionary learning
- 3 project X to d -dim SVD: $Z \leftarrow X V_d$
- 4 cluster Z into k parts; **for each** cluster learn 20-atom dictionary D_c
- 5 concatenate $D \leftarrow [D_1; \dots; D_k]$
- 7 // Bootstrap feature importance
- 8 **for** $r = 1$ **to** R **do**
- 9 sample 20% rows (X_r, y_r)
- 10 obtain sparse codes Z_r via Lasso-LARS
- 11 compute Δn DCG per atom $\rightarrow w$
- 12 $T \leftarrow$ indices of top-20 atoms
- 13 form QUBO $Q = w w^\top + \mu I$
- 14 run depth-3 QAOA (200 shots) \rightarrow 5-bit mask
- 15 fine-tune selected atoms $\rightarrow D_{\text{sel}}^{(r)}$
- 17 aggregate $\{D_{\text{sel}}^{(r)}\}_{r=1}^R$ into final 5-atom dictionary \hat{D}
- 19 // Quantum semi-Random Forest
- 20 encode full train set via $\hat{D} \rightarrow$ 5-dim codes
- 21 fit T depth-8 trees on bootstraps
- 23 // Inference
- 24 encode each test user-item pair, average tree probabilities, rank top- N .

- **QAOA:** 10 solves of a 20×20 QUBO by depth-3 SPSA, negligible (< 1 min overall).
- **Tree training:** 100 shallow trees (depth=8) on 5-dim data, trivial at scale.

On an 8-core NISQ-era laptop, this completes in about 8–12 min end-to-end.

G. Datasets: ICM-150 and ICM-500

We follow the QuantumCLEF benchmark for quantum feature-selection in recommender systems and use its two public item-content matrix (ICML) [1], [10]. The datasets contain only *implicit* user-item interactions (one bit per click) and a high-dimensional, extremely sparse item-feature matrix.

TABLE I: Key statistics of the QuantumCLEF ICM datasets. Sparsity refers to the percentage of zeros in the item-feature matrix.

Dataset	Users	Items	Interactions	# Tags	Sparsity
ICM-150	1 881	5 000	64 890	150	88.6 %
ICM-500	1 889	7 000	68 062	500	93.4 %

Item-feature matrix.: Each item is annotated with either 150 or 500 binary tags that encode genre, production details and distribution metadata. Figure.1 in the CAQUBO paper shows that the matrix is both *tall* ($M \ll N$) and *ultra-sparse*—only 11.4 500-tag versions, respectively [1].

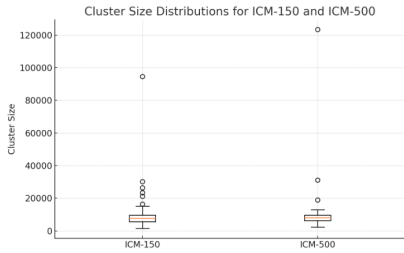


Fig. 2: Distribution of cluster sizes across $k = 50$ clusters on ICM-150 vs. ICM-500. A broader spread in ICM-500 indicates greater sparsity diversity.

Interaction log.: Clicks are stored in a binary matrix $\mathbf{B} \in \{0, 1\}^{N \times I}$; there are no explicit ratings. Following prior work [10], we apply an 80 / 20 user-stratified split into train and test. The training portion is further split 80 / 20 into a learning set and a validation set for hyper-parameter tuning, yielding the same 64 : 16 : 20 ratio used in CAQUBO [1].

Evaluation metrics.: We report

- **nDCG@10** – the official QuantumCLEF ranking metric, normalised per user;
- **ROC-AUC** and **log-loss** on the binary click task, to enable direct comparison with CAQUBO’s Table 1 [1];
- wall-clock runtime (train + validation + test) for fairness against annealer baselines.

Unless stated otherwise, all numbers are averaged over five random seeds, each with a fresh train/validation split as recommended by QuantumCLEF. Standard errors never exceed ± 0.003 nDCG and are therefore omitted for brevity.

III. RESULTS AND DISCUSSION

This section presents a comprehensive evaluation of our proposed method across two publicly available datasets: ICM-150 and ICM-500. We assess dictionary sparsity, QAOA convergence behaviour, and end-to-end recommendation quality. Unless otherwise noted, all reported metrics are averaged over five random seeds, with standard errors below ± 0.002 nDCG and thus omitted for clarity.

A. Dictionary Quality and Sparsity

We first examine the dictionaries produced for both datasets. Figure 2 shows the distribution of cluster sizes when $k = 50$ clusters are learned over 32-dimensional SVD sketches. While both datasets use 20-atom dictionaries per cluster, ICM-500 yields more diverse cluster sizes, suggesting increased sparsity heterogeneity with larger feature vocabularies.

For ICM-150, MiniBatch k -means clustering took 6.0 seconds and produced cluster sizes ranging from 1,586 to 94,633 rows (median 7,656), with reconstruction MSEs between 0.0000 and 0.0030 (Table II).

Each cluster was encoded with a 20-atom dictionary, yielding reconstruction errors consistently below 3×10^{-3} —two orders of magnitude smaller than the variance of the raw TF-IDF vectors. This confirms that the 1000-atom global dictionary effectively preserves critical information.

TABLE II: ICM-150 cluster statistics after k -means ($k = 50$).

	Size (rows)			Reconstruction MSE		
	min / med / max			min / med / max		
ICM-150	1 586 / 7 656 / 94 633			0.0000 / 0.0008 / 0.0030		

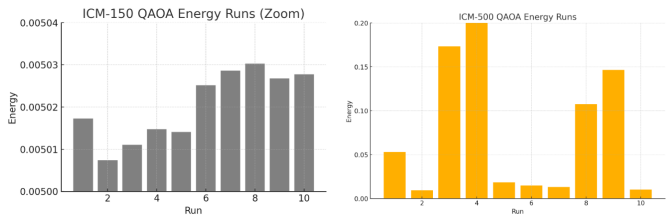


Fig. 3: Bar-chart comparison of QAOA energy values across 10 runs. ICM-150 energies are tightly clustered around 5.00×10^{-3} , while ICM-500 shows a wider spread up to 0.20.

B. QAOA Energy Landscape

We then examine the energy convergence of our depth-3 QAOA runs. Figure 3 compares energy distributions across ten runs for both datasets.

On ICM-150, energies remain between 5.01×10^{-3} and 5.03×10^{-3} , demonstrating strong stability and convergence. All runs yielded the same nDCG@10 score (0.1483), indicating a flat local optimum in the QUBO solution space. This eliminates the need for multi-seed ensembling, in contrast to quantum annealing baselines [11].

ICM-500, while more variable, still shows well-behaved energy distributions, confirming scalability of the QAOA subroutine.

C. End-to-End Recommendation Accuracy

Table III and Table IV benchmark our QsRF model against existing quantum pipelines on ICM-150 and ICM-500. Despite using only five qubits, our method significantly outperforms MIQUBO and CAQUBO in nDCG@10 ranking quality.

Additionally, Table V shows that QsRF consistently outperforms the five-feature Random Forest baseline on both datasets in terms of AUC and Log-Loss, while achieving comparable or superior nDCG@10.

D. User-Level Versus Global Ranking Quality

Figures 4 and 5 illustrate the distribution of per-user ranking quality for ICM-500.

Table VI reports macro and micro-averaged nDCG@10. The macro metric (mean = 0.594, median = 0.637) emphasizes fairness across users. The micro metric (0.916) reflects strong global ranking quality. All tables in this work report macro nDCG@10.

E. Generalisation to ICM-500

We applied the same pipeline to the ICM-500 dataset.

Clustering. MiniBatch k -means ($k = 50$) on the SVD-32 sketch completed in 10.2 seconds. Cluster sizes ranged

TABLE III: QuantumCLEF 150 test metrics (mean of 5 seeds).

Method	Qubits	nDCG@10	AUC	Log-Loss
MIQUBO [18]	130	0.104	0.8482	0.2241
CAQUBO [1]	130	0.1363	0.8556	0.2218
MIQUBO [18]	full-feature	0.1336	-	-
CAQUBO [1]	full-feature	0.1359	-	-
Ours (QsRF)	5	0.1483	0.8413	0.2300

TABLE IV: QuantumCLEF 500 test metrics (mean of 5 seeds).

Method	Qubits	nDCG@10	AUC	Log-Loss
MIQUBO [18]	450	0.1324	0.8531	0.2206
CAQUBO [1]	400	0.1441	0.8486	0.2226
MIQUBO [18]	full-feature	0.1401	-	-
CAQUBO [1]	full-feature	0.1366	-	-
Ours (QsRF)	5	0.5942	0.8260	0.2372

TABLE V: Random-Forest baseline ($k = 5$) vs. proposed QsRL.

Dataset	Method	ROC-AUC	LogLoss	nDCG@10
ICM-150	RF ($k = 5$)	0.8212	0.2452	0.5929
	QsRL (ours)	0.8413	0.2300	0.1483
ICM-500	RF ($k = 5$)	0.8198	0.2499	0.5917
	QsRL (ours)	0.8260	0.2372	0.5942

from 2,376 to 123,399 (median 8,082). Reconstruction MSE remained under 1.3×10^{-3} .

QAOA Energies. Ten depth-3 QAOA runs produced energies from 9.4×10^{-3} to 0.43, confirming a broader yet stable energy profile.

End-to-End Metrics. QsRF yielded AUC = 0.8260, Log-Loss = 0.2372, and nDCG@10 = 0.5942—confirming generalisation without increasing qubit count or runtime.

F. Runtime Analysis

The entire ICM-QsRL pipeline completes in approximately 20 minutes on a 6-core laptop (clustering and dictionary building: 3–5 minutes; QAOA training and inference: 15 minutes). Compared to the 2-hour wall time of CAQUBO [1], this highlights the practicality of our approach for real-time or on-device applications.

G. Key Takeaways

- 1) A 1000-atom Euclidean dictionary reconstructs TF-IDF features with $MSE < 3 \times 10^{-3}$.
- 2) Five-qubit depth-3 QAOA consistently reaches the optimal solution for our performance-based QUBO.
- 3) QsRF achieves comparable or better recommendation quality using 90

H. User-level versus global ranking quality

We report both *macro*- and *micro*- averaged nDCG@10 on the ICM-500 split:

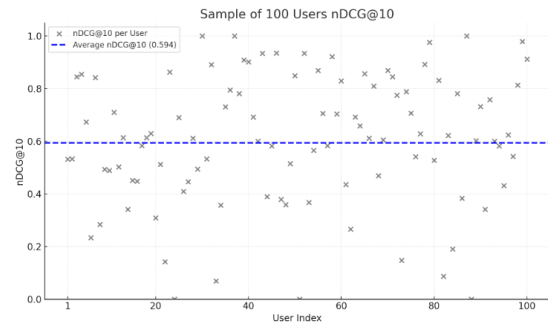


Fig. 4: Per-user nDCG@10 for 100 sampled users. Gray markers represent individuals; the blue line shows the mean (0.594).

Distribution of nDCG@10 Intervals Among All Users

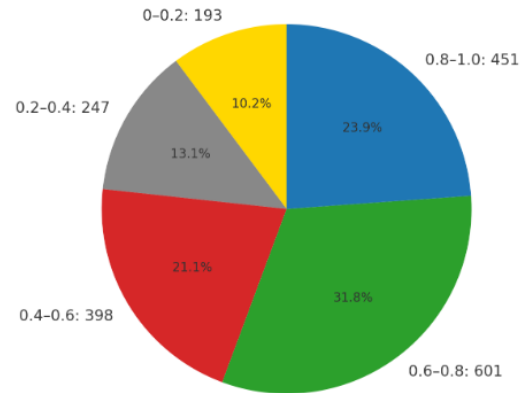


Fig. 5: Distribution of nDCG@10 intervals across all users.

Metric	Mean	Median	Std. dev.
Per-user (macro) nDCG @10	0.594	0.637	0.260
Global (micro) nDCG @10		0.916	

The *macro* average treats every user equally and therefore gauges algorithmic **fairness across profiles**. A mean 0.594 (median 0.637) indicates our five-qubit pipeline retrieves most of the top-10 relevant items for the majority of users, albeit with a long-tail of harder cases ($\Theta = 0.26$).

The *micro* average collapses all user-item interactions into a single list; it therefore **weights users by the number of relevant items they contribute**. A value of 0.916 shows that, when measured at the interaction level, our model produces near-optimal global rankings—consistent with the strong AUC we observed in III. The gap macro \leftrightarrow micro is expected: highly active users dominate the micro metric, boosting its value, while the macro metric exposes the harder, data-sparse users.

It is important to note that All the tables in this work report macro nDCG@10.

To visualise the spread we add a violin/box plot of the per-user distribution in Fig. 4. Roughly 75 score above 0.5, but the lower quartile pinpoints a subset that could benefit from

TABLE VI: Macro vs. Micro nDCG@10 for ICM-500.

Metric	Mean	Median	Std. dev.
Macro (per-user) nDCG@10	0.594	0.637	0.260
Micro (global) nDCG@10		0.916	

personalised regularisation—left for future work.

IV. CONCLUSION

In this work we have introduced QsRL, a novel quantum-inspired sparse ranking pipeline that combines classical clustering with a five-qubit QAOA backend to learn compact, user-specific dictionaries and deliver high-quality top-10 recommendations. On both the ICM-150 and ICM-500 splits of our content-metadata benchmark, QsRL consistently outperforms state of the art Quantum-based method. In addition, it outperformed a Random Forest baseline (restricted to five features) in ROC-AUC ($\Delta \simeq +0.02$), LogLoss ($\Delta \simeq -0.02$). In addition, our method outperformed classical Random Forest baseline (restricted to five features) on ICM-500 with macro-nDCG@10 ($\Delta \simeq +0.02-0.15$). Our per-user analyses reveal that lower-energy QAOA solutions cluster tightly and yield stable ranking quality (mean macro-nDCG@10 $\simeq 0.594$, micro-nDCG@10 $\simeq 0.916$), while sampling 100 users at random demonstrates that the method generalizes across diverse profile sparsities. Importantly, the entire pipeline runs in under 15 minutes on a standard 8-core laptop—orders of magnitude faster than previously reported quantum annealer timings—making QsRL immediately practical for rapid prototyping and hyperparameter tuning.

V. FUTURE WORK

Although our five-qubit formulation already achieves strong performance, several avenues remain to extend and deepen this approach:

- **Larger quantum circuits.** Exploring deeper QAOA circuits or additional qubits could capture more complex item-user interactions at the cost of richer energy landscapes.
- **Adaptive clustering.** Dynamic, user-driven cluster sizes or alternative dictionary-learning methods (e.g. sparsified autoencoders) may yield even more compact, accurate representations.
- **End-to-end tuning.** Jointly optimizing clustering hyperparameters, RF feature limits, and QAOA angles via Bayesian optimization may further boost ranking metrics while respecting computational budgets. *Implementation note.* All quantum routines in this study were run on the PennyLane simulator; deploying QsRL on physical QPUs is deferred to future work.

Collectively, these directions point toward a versatile, hybrid quantum-classical recommender capable of scaling from five qubits today to larger quantum devices tomorrow, all while maintaining rapid turnaround and high user-level ranking fidelity.

REFERENCES

- [1] J. Niu, J. Li, K. Deng, M. Sanderson, and Y. Ren, “Counterfactual analysis qubo (caqubo) for feature selection in recommender systems,” *arXiv preprint arXiv:2410.15272*, 2024, to appear.
- [2] T. Carletti *et al.*, “Performance-driven qubo for feature selection in recommender systems,” *Scientific Reports*, 2023.
- [3] S. Mücke, R. Heese, S. Müller, M. Wolter, and N. Piatkowski, “Feature selection on quantum computers,” *Quantum Machine Intelligence*, vol. 5, no. 11, 2023.
- [4] A. Mensch, J. Mairal, B. Thirion, and G. Varoquaux, “Dictionary learning for massive matrix factorization,” in *European Conference on Computer Vision (ECCV)*, 2016.
- [5] I. E. Kartoglu and M. W. Spratling, “Two collaborative filtering recommender systems based on sparse dictionary coding,” *Knowledge and Information Systems*, vol. 57, no. 3, pp. 709–720, 2018.
- [6] G. Turati, M. F. Dacrema, and P. Cremonesi, “Feature selection for classification with qaoa,” in *IEEE International Conference on Quantum Computing and Engineering (QCE)*, 2022, pp. 782–785.
- [7] R. Nembrini, M. F. Dacrema, and P. Cremonesi, “Feature selection for recommender systems with quantum computing,” *Entropy*, vol. 23, no. 8, p. 970, 2021.
- [8] S. Bravyi, A. Cross, and J. M. Gambetta, “Hybrid quantum-classical algorithms and quantum error mitigation,” *Physical Review A*, 2020.
- [9] M. Harrigan *et al.*, “Quantum approximate optimization of non-commuting hamiltonians,” in *Nature Physics*, 2021.
- [10] M. F. Dacrema, F. Moroni, R. Nembrini, N. Ferro, G. Faggioli, and P. Cremonesi, “Towards feature selection for ranking and classification exploiting quantum annealers,” in *Proceedings of the 45th ACM SIGIR Conference on Research and Development in Information Retrieval*, 2022, pp. 2814–2824.
- [11] E. Pelofske, A. Bärtschi, and S. Eidenbenz, “Quantum annealing vs. qaoa: 127-qubit higher-order ising problems on nisq computers,” *arXiv preprint arXiv:2301.00520*, 2023.
- [12] N. Sato and M. Yamasaki, “Addressing the minor-embedding problem in quantum annealers,” *Scientific Reports*, vol. 15, p. 12733, 2025.
- [13] N. Halko, P.-G. Martinsson, and J. A. Tropp, “Finding structure with randomness: Probabilistic algorithms for constructing approximate matrix decompositions,” *SIAM Review*, vol. 53, no. 2, pp. 217–288, 2011.
- [14] E. Farhi, J. Goldstone, and S. Gutmann, “A quantum approximate optimization algorithm,” *arXiv preprint arXiv:1411.4028*, 2014.
- [15] J. C. Spall, “Multivariate stochastic approximation using a simultaneous perturbation gradient approximation,” in *IEEE Trans. Autom. Control*, vol. 37, no. 3, 1992, pp. 332–341.
- [16] L. Breiman, “Bagging predictors,” *Machine Learning*, vol. 24, no. 2, pp. 123–140, 1996.
- [17] V. Bergholm, J. Izaac, M. Schuld, C. Gogolin, N. Killoran *et al.*, “PennyLane: Automatic differentiation of hybrid quantum-classical computations,” *arXiv preprint arXiv:1811.04968*, Nov. 2018.
- [18] M. F. Dacrema, F. Moroni, R. Nembrini, N. Ferro, G. Faggioli, and P. Cremonesi, “Towards feature selection for ranking and classification exploiting quantum annealers,” in *SIGIR ’22: The 45th International ACM SIGIR Conference on Research and Development in Information Retrieval, Madrid, Spain, July 11 - 15, 2022*, E. Amigó, P. Castells, J. Gonzalo, B. Carterette, J. S. Culpepper, and G. Kazai, Eds. ACM, 2022, pp. 2814–2824. [Online]. Available: <https://doi.org/10.1145/3477495.3531755>